



Supporting Online Material for

Functional Proteomics Identify Cornichon Proteins as Auxiliary Subunits of AMPA Receptors

Jochen Schwenk,¹ Nadine Harmel,¹ Gerd Zolles,¹ Wolfgang Bildl,¹ Akos Kulik,⁴
Bernd Heimrich,⁴ Osamu Chisaka,⁶ Peter Jonas,³ Uwe Schulte,^{1,2}
Bernd Fakler,^{1,5*} Nikolaj Klöcker^{1*}

*To whom correspondence should be addressed. E-mail: bernd.fakler@physiologie.uni-freiburg.de (B.F.) or nikolaj.kloecker@physiologie.uni-freiburg.de (N.K.)

Published 6 March 2009, *Science* **323**, 1313 (2008)
DOI: 10.1126/science.1167852

This PDF file includes

Materials and Methods
Figs. S1 to S7
Table S1
References

Supporting Online Material

Materials and methods

Molecular biology

Preparation and injection of cRNAs into *Xenopus* oocytes was done as described (1). All cDNAs were verified by sequencing; genebank accession numbers of the clones used are NM_001025132 (CNIH-2), FJ403327 (CNIH-3), GluR-A_i (flip variant of GluR-A, M38060.1), GluR-A_o (flop variant of GluR-A, NM_031608.1), GluR-B_i (NM_017261.2), GluR-B_o (NP_001077280.1), GluR-D_o (NM_017263.1), NM_053351 (TARP γ -2).

Biochemistry

Plasma membrane-enriched protein fractions were prepared from freshly isolated adult rat (Wistar, \geq P30) brains as described (2) and solubilized at 4°C in 1 mg/ml ComplexioLyte buffer with protease inhibitors added and cleared by ultracentrifugation (30 min at 125.000 x g).

BN-PAGE. For two-dimensional gel electrophoresis, protein complexes were solubilized with ComplexioLyte48 (salt replaced by 0.5 M betaine), centrifuged on a sucrose gradient (400,000 x g, 60 min, 4°C), supplied with Coomassie G250 (0.05% final concentration) and loaded on a linear 3-15% polyacrylamide gel. A mixture of native proteins was run as a standard for complex size in the first dimension. The gel buffer contained 50 mM BisTris (pH 7.5), 0.5 M betaine, 1 mM EDTA, 0.25% detergent of ComplexioLyte48. The cathode chamber was filled with 15 mM BisTris, 0.05 mM Tricine, 0.01% Coomassie G250, the anode buffer was 15 mM BisTris (pH 7). After equilibration in Laemmli buffer, excised BN-PAGE lanes were placed on a 15% SDS-PAGE gel (with a 4% stacking gel) for separation in the second dimension. For antibody shift experiments, 150 μ g of solubilized complexes were pre-incubated for 30 minutes with 5 μ g *anti- γ -2/3* (for target specificity see Fig. S2B) or 5 μ g *anti-CNIH-2/3* (for target specificity see Fig. S2A), respectively, prior to the addition of Coomassie G250. After electroblotting of SDS-PAGE-resolved samples on PVDF membrane, the blot was split into three molecular weight ranges and subjected to separate Western analysis with mouse *anti-GluR-B*, rabbit *anti- γ -2/3* and rabbit *anti-CNIH-2/3*; antibody-stained proteins were visualized by *anti-mouse* or *anti-rabbit* IgG-HRP and ECL Plus.

Affinity purification. Solubilized material (3 mg, ComplexioLyte48 and 91) was incubated for 2 hours at 4°C with 20 μ g immobilized affinity-purified rabbit *anti-GluR-A*, mouse *anti-GluR-B*, rabbit *anti- γ -2/3* and rabbit *anti-CNIH-2/3* or control IgG pools. After brief washing, bound proteins were eluted with Laemmli buffer

(DTT added after elution). Prior to tryptic digestion eluates were shortly run on SDS-PAGE gels and silver stained.

Probing protein-protein interaction in Xenopus oocytes. Oocytes (4 days after injection of cRNA) were homogenized with potters in 0.5 ml solution (pH adjusted to 7.4) containing 10 mM HEPES, 83 mM NaCl, 1 mM MgCl₂, 1 mM EGTA, 1 mM iodoacetamide (with protease inhibitors) and centrifuged for 10 min at 100 x g and 300 x g to remove yolk and nuclear material. Supernatants were subjected to ultracentrifugation (30 min at 125,000 x g) to obtain crude membrane preparations. Membranes (from 20 oocytes) were solubilized using ComplexioLyte48 and subjected to analytical APs (5 µg antibody).

Standards for MS quantification. GFP-tagged fusions of CNIH-2 and γ -2 were overexpressed in cultured tsA-cells. 2 days after transfection, cells were lysed and homogenized with glass potters and ultrasonication in 500 µl 20 mM Tris/HCl (pH 7.4), 150 mM NaCl, 1 mM EDTA (protease inhibitors added). Homogenates were centrifuged for 3 min at 1,000 x g and crude membranes were obtained by ultracentrifugation (30 min at 125,000 x g). After solubilization with ComplexioLyte48, target proteins were affinity-purified with an *anti-GFP* antibody as described above. Eluates were diluted and mixed to obtain an equimolar standard solution of γ -2 and CNIH-2 using intensities of the *anti-GFP* Western signals (see below).

Mass spectrometry

Protein samples were in-gel digested with trypsin as described previously (3). Extracted peptides were re-dissolved in 0.5% trifluoroacetic acid and loaded on a C18 PepMap100 precolumn (5 µm) using an UltiMate 3000 HPLC. Peptides were eluted with an aqueous-organic gradient, resolved on a 75 µm column (tip: 8 ± 1 µm) packed with ReproSil-Pur 120 ODS-3 (C18; 3 µm; Dr. A Maisch, Ammerbuch-Entringen, Germany) and directly electrosprayed into an LTQ-FT mass spectrometer as described earlier (3). Each scan cycle consisted of one FTMS full scan and up to five ITMS dependent MS/MS scans of the five most intense ions. Dynamic exclusion (30 sec, mass width 20 ppm) and monoisotopic precursor selection were enabled. Extracted MS/MS spectra were searched against the Swissprot or NCBI nr database (Mammalia) using the Mascot search engine accepting common variable modifications and one missed tryptic cleavage. Peptide tolerance was ± 10 ppm and MS/MS tolerance was ± 0.8 Da.

MS data were evaluated by three different approaches:

(i) The relative peptide query (rPQ) score as detailed in (3) is a measure for the specificity of a protein identified in a given AP; rPQ scores > 4 are indicative for specific co-purification (3).

(ii) The normalized PQ score (PQ_{norm}) is defined as the ratio of all PQs (sum of all MS/MS spectra) obtained for any given protein and the number of peptides theoretically identifiable for this protein in MS analyses (6-25 amino acids in length); the PQ_{norm} score is a quantitative measure for the coverage (and hence the abundance) of a given protein in a sample.

(iii) More accurate quantification was achieved by extraction of LC-MS peak volumes (integral of m/z signals, also termed total ion current, XIC) that are directly proportional to the abundance of a peptide fragment (calculated with *msInspect*, Computational Proteomics Laboratory, Fred Hutchinson Cancer Research Center, Seattle, WA, USA). For normalizing the XIC of peptide precursor ions unique for CNIH-2 and γ -2 (Fig. 2B), an equimolar mixture of these proteins fused to GFP was analyzed by LC-MS/MS; deviations from the adjusted 1:1 stoichiometry (estimated by *anti-GFP* Western signal intensities) were corrected by using GFP-specific peptides as internal standards. Two peptide ions consistently measured over the dilution range tested (Fig. 2B, upper panel) were used for calibration of molar ratios. Relative amounts of the four GluR subunits in the different APs were determined by relative quantification of subunit-specific peptide signals and normalization to signal ratios of peptides common to all four subunits (intensity-weighted averages of 3-7 peptide ion XIC ratios each).

Immunocytochemistry and surface labeling

HeLa cells were grown in DMEM supplemented with 10% fetal calf serum, 1% HEPES, and 1% penicillin/streptomycin at 37°C and 5% CO₂. At ~80% confluence, cells were transfected with the respective cDNAs using Fugene HD Transfection Reagent following the supplier's instructions. For immunocytochemistry, transfected cells were fixed in 4% paraformaldehyde in phosphate buffered saline (PBS), pre-treated with 10% normal goat serum (NGS) in PBS with 0.04% Triton X-100 (PBS-T) for 1 h, and incubated with rabbit polyclonal *anti-CNIH-2/3* antiserum (1:500 in 2% NGS/PBS-T; (4)) for 1 h at room temperature. Immunoreactivity was visualized by goat *anti-rabbit* antiserum conjugated to cy-3 (1:500 in 10% NGS/PBS-T). For selective detection of AMPARs on the cell surface, an extracellular epitope tagging approach was employed. Confluent HeLa cells expressing AMPARs assembled from GluR-A_i that harbour a hemagglutinin (HA) epitope at their N-terminus (kindly provided by P. Osten, Northwestern University, Chicago) were processed for *anti-HA* immunoreactivity without detergents. Cells were incubated in mouse monoclonal *anti-HA* antiserum (1:100 in PBS) followed by goat *anti-mouse* antiserum conjugated to horseradish peroxidase (1:5000 in 10% NGS/PBS). Immunoreactivity was detected by

enzymatic turnover of SuperSignal ELISA substrate and quantified in a Glomax 20/20n luminometry system.

Immunohistochemistry

Anaesthetized Wistar rats (P30) were transcardially perfused with PBS followed by 4% PFA/PBS for 10 min. Brain tissues were post-fixed in 4% PFA/PBS at 4 °C for 5 hrs. Horizontal sections (50 µm) cut on a vibratome were blocked in 5% NGS/PBS-T for 1 h at room temperature and incubated in rabbit polyclonal *anti-CNIH-2/3* antiserum (1:500 in PBS-T) at 4 °C overnight. CNIH-2/3 immunoreactivity was visualized by goat *anti-rabbit* antiserum conjugated to cy-3 (1:1000 in 10% NGS/PBS-T). For control experiments, the primary antiserum was omitted. Glial cell populations were identified by mouse monoclonal *anti-glia fibrillary acidic protein* (GFAP) antiserum (1:200 in PBST) visualized by goat *anti-mouse* antiserum conjugated to cy-2 (1:1000 in 10 % NGS/PBS-T). Cell nuclei were counterstained with 4',6-Diamidino-2-phenylindol (DAPI). Sections were imaged with a Zeiss ApoTome microscope.

Electron microscopy

Post-embedding immunogold EM was performed as described earlier (5). Reactions were performed on 95-nm-thick sections of slam-frozen, freeze-substituted, lowicryl-embedded CA1 area of the hippocampus. Sections were picked up on glue-coated 100-mesh grids. Subsequently, they were incubated in 50 mM Tris-buffered saline (TBS) containing 0.1% Triton X-100 (TBST), 0.1% sodium borohydride and 50 mM glycine for 10 min, in TBST containing 2% human serum albumin (HSA) for 30 min, and then with *anti-CNIH-2/3* (in TBST containing 2% HSA) for 3 h at room temperature. After washing in TBST and blocking in 2% HSA in TBST, sections were incubated with goat anti-rabbit IgG coupled to 10 nm gold particles (diluted 1:30) in TBST containing 2% HSA and 5mg/ml polyethylene glycol for 2 h at room temperature. After several washes in TBS and distilled water, sections were counterstained with saturated aqueous uranyl acetate followed by staining with lead citrate.

Electrophysiology and data analysis

Electrophysiological recordings from whole oocytes or from giant outside-out patches excised from oocytes were performed at room temperature (22-24 °C) as described previously (3, 6). Briefly, two-electrode voltage-clamp recordings from whole oocytes were performed with a TurboTec 01C amplifier, using microelectrodes of 0.1-0.5 MΩ resistance filled with 3 M KCl and a bath chamber perfusion achieving solution exchanges within ~1 s; holding potential was -50 mV.

In excised patch experiments, currents were recorded with an EPC9 amplifier, low-pass filtered at 3 kHz, and sampled at 5-10 kHz. Pipettes made from thick-walled borosilicate glass had resistances of 0.4-0.8 M Ω when filled with intracellular solution (K_{int} ; in mM) 120 KCl, 5 HEPES, 10 EGTA, pH adjusted to 7.2. Extracellular solution (K_{ext}) applied to outside-out patches was composed as follows (mM): 120 KCl, 5 HEPES, 1.3 mM CaCl₂ (pH 7.2). Rapid application/removal of glutamate (1 mM, dissolved in K_{ex}) was performed using a Piezo-controlled fast application system with a double-barrel application pipette that enables solution exchanges within less than 100 μ s (20-80%, measured from the open tip response during a switch between normal and 10x-diluted K_{ext}).

Deactivation, desensitization and recovery from desensitization of AMPARs were characterized by time constants derived from mono- (three free parameters) or bi-exponential fits (five free parameters) to the decay phase or recovery of the glutamate-activated currents; the quality of the fit result was judged from the sum of squared differences value. For the deactivation time course of the different types of AMPAR complexes, bi-exponential fits were considered valid if the relative amplitude of the slow component was > 5% and the slow component was consistently identified (in > 75% of patches of the respective data set). Curve fitting and further data analysis were done with Igor Pro 4.05A Carbon. Data in text and figures are given as mean \pm SD, unless specified differently.

Simulations of EPSPs

Simulations of EPSPs (Fig. S6) were performed as described previously (7, 8). CA3 pyramidal neurons were chosen, as these cells express AMPARs of the GluR-A_i/B_i-type (9), similar to the recombinant AMPARs primarily examined in the present study (Figs. 5 and 6). A biocytin-filled and reconstructed CA3 pyramidal neuron (CA3_15 from a previously published sample (7)) was used for analysis of EPSP time course and temporal summation. For the cell chosen, the cable parameters were $R_i = 294 \text{ W cm}$, $R_m = 164000 \text{ W cm}^2$, and $C_m = 0.683 \text{ }\mu\text{F cm}^2$. Simulations were performed using NEURON 6.1 (10). The time step was 5 μ s in all simulations.

Supplementary Figures

Fig. S1

Two-dimensional gel separation of AMPAR complexes from rat brain as in Figure 1, Western-probed with the *anti-GluR-B*, *anti- γ -2/3* and *anti-GluR-A* antibodies. Size (BN-PAGE, derived from standards for high molecular weight complexes) and molecular weight (SDS-PAGE) as indicated.

Fig. S2

Characterization of the *anti-CNIH-2/3* (A) and *anti- γ -2/3* (B) antibodies.

(A) CNIH isoforms 1-4 were expressed as GFP-fusion proteins in opossum kidney cells (left panel, GFP-fluorescence) and stained with the *anti-CNIH-2/3* antibody (middle panel); right panel is the merge of left and middle panels. Note that *anti-CNIH-2/3* recognizes both CNIH-2 and CNIH-3. (B) SDS-PAGE separation of solubilisates and eluates of APs with *anti- γ -2/3* on membrane fractions prepared from wildtype (WT) and *stargazer* (Star) mice; blots were Western-probed with the indicated antibodies. (C) GluR, TARP and CNIH proteins affinity-purified with the *anti- γ -2/3* antibody from the aforementioned membrane fractions and identified by nano-LC MS/MS analyses. MS procedures and scores as in Table 1.

Note that the *anti- γ -2/3* antibody effectively purified γ -3 (together with all GluR, TARP and CNIH proteins) from both WT and *stargazer* mice and recognized the denatured γ -3 protein in the Western blots.

Fig. S3

Solubilization efficiency of the GluR, CNIH and TARP proteins.

(A) SDS-PAGE separation of solubilized (S) and non-solubilized (pellet, P) protein fractions obtained with ComplexioLytes48 (Sol A) and 91 (Sol B) from rat brain membranes. Protein separations were Western-probed with the indicated antibodies. (B) Bar graph illustrating solubilization efficiency of the GluR-A, GluR-B, CNIH-2/3 and γ -2/3 proteins as determined by densitometric analysis of the Western blots in (A).

Fig. S4

Two-dimensional gel separation of AMPAR complexes from rat brain without (upper panel, control conditions) and with the *anti-CNIH-2/3* antibody (lower panel, antibody-shift assay) added to the solubilized membrane fraction; subsequently, the gel separations were Western-probed with the indicated antibodies. Size (BN-PAGE) and molecular weight (SDS-PAGE) as indicated. Red lines indicate

position of the CNIH proteins in control conditions (dotted line) and in the shift-assay (continuous line). Note that in the shift-assay no AMPAR signal could be detected at the location where a prominent signal was observed under control conditions; this indicated that all AMPARs not associated with the TARPs are co-assembled with the CNIH proteins.

Fig. S5

Comparison of gating kinetics of recombinant AMPAR-CNIH complexes with native AMPARs expressed in hippocampal neurons.

(A) AMPAR-mediated currents from five different hippocampal hilar mossy cells evoked by 1-ms (left panel) and 100-ms pulses of 1 mM glutamate (right panel). Glutamate was rapidly applied to oo-patches isolated from neurons in rat hippocampal slices (P12 - 17) via a Piezo-driven application system. Traces were normalized to the same peak value to facilitate comparison of the decay time course. AMPARs from these hippocampal neurons are mainly assembled from GluR-A_i and GluR-B_i subunits (as determined by single-cell RT-PCR subsequent to oo-patch experiments; (9)). Red traces were recorded from the same oo-patch. (B, C) Bar graph illustrating the values of $\tau_{\text{deactivation}}$ (B) and $\tau_{\text{desensitization}}$ (C) obtained by monoexponential fits to the decay of currents evoked by 1-ms or 100-ms glutamated pulses in native AMPARs expressed in hilar mossy cells and CA3 pyramidal neurons (data were taken from (9)) and in recombinant AMPARs assembled in *Xenopus* oocytes upon injection of GluR-A_i, GluR-B_i and CNIH-2 cRNAs at the indicated ratios. For recombinant AMPARs expressed from GluR-A_i/B_i + CNIH-2 cRNA injections at a 1 / 1 ratio the deactivation time course could not be adequately fitted with a monoexponential function (see text).

Fig. S6

CNIH-mediated alterations of postsynaptic AMPAR kinetics changes timing, efficacy, and temporal summation of glutamatergic synaptic transmission.

(A) Simulation of local EPSPs (red traces) and somatic EPSPs (black traces) in a CA3 pyramidal neuron for excitatory synapses at three different locations. Left panel, decay time constant ($\tau_{\text{deactivation}}$) of synaptic conductance = 1 ms (corresponding to the deactivation time constant of GluR-A_i/B_i AMPARs); right panel, decay time constant of synaptic conductance = 7.5 ms (representing the mean deactivation time constant (approximation with a monoexponential function) of GluR-A_i/B_i AMPARs associated with CNIH-2 or CNIH-3). Local and somatic EPSPs were normalized to the same peak value to facilitate comparison of kinetics.

(B - D), Time-to-peak (B), amplitude-weighted average decay time constant (C), and peak amplitude (D) of local EPSP (filled symbols) and somatic EPSPs (open symbols) as a function of the decay time constant of the synaptic conductance ($\tau_{\text{deactivation}}$).

(E, F) Temporal summation of two EPSPs generated at variable time intervals. (E) Traces of EPSPs with rapidly decaying synaptic conductance (left) and slowly decaying synaptic conductance (right); interevent interval 20 ms. (F) Plot of paired pulse ratio as a function of interevent interval. The curve series corresponds to values of $\tau_{\text{deactivation}}$ varied between 0.5 and 7.5 ms in 0.5 ms steps.

In panels (B) to (F), the synapse was placed on the proximal apical dendrite. For all computations, a detailed passive cable model of a CA3 pyramidal neuron was used (CA3_15 from a previously reconstructed sample of cells; (7)). Synaptic rise time constant, 0.2 ms; peak conductance, 2 nS; reversal potential -5 mV.

Table S1.

Glur, TARP and CNIH proteins affinity-purified with the indicated antibodies from rat brain membrane fractions and identified by nano-LC MS/MS analyses. Procedures used for APs and mass spectrometry are detailed above. rPQ is relative peptide query score; values for rPQ > 4 indicate specific co-purification of a given protein (3). PQ_{norm} is normalized peptide query score; the values for PQ_{norm} are quantitative measures for the coverage (and hence the abundance) of a given protein in an AP.

References

1. B. Fakler *et al.*, *Cell* **80**, 149 (1995).
2. C. A. Sailer *et al.*, *J Neurosci* **22**, 9698 (2002).
3. H. Berkefeld *et al.*, *Science* **314**, 615 (2006).
4. H. Hoshino *et al.*, *Mol Biol Cell* **18**, 1143 (2007).
5. A. Kulik *et al.*, *Eur J Neurosci* **15**, 291 (2002).
6. D. Oliver *et al.*, *Mol Pharmacol* **60**, 183 (2001).
7. G. Major, A.U. Larkman, P. Jonas, B. Sakmann, J.J. B. Jack, *J Neurosci* **14**, 4613 (1994).
8. C. Schmidt-Hieber, P. Jonas, J. Bischofberger, *J Neurosci* **27**, 8430 (2007).
9. J. R. P. Geiger *et al.*, *Neuron* **15**, 193 (1995).
10. N. T. Carnevale, M. L. Hines, *The Neuron book*. (Cambridge University press, Cambridge, 2006).

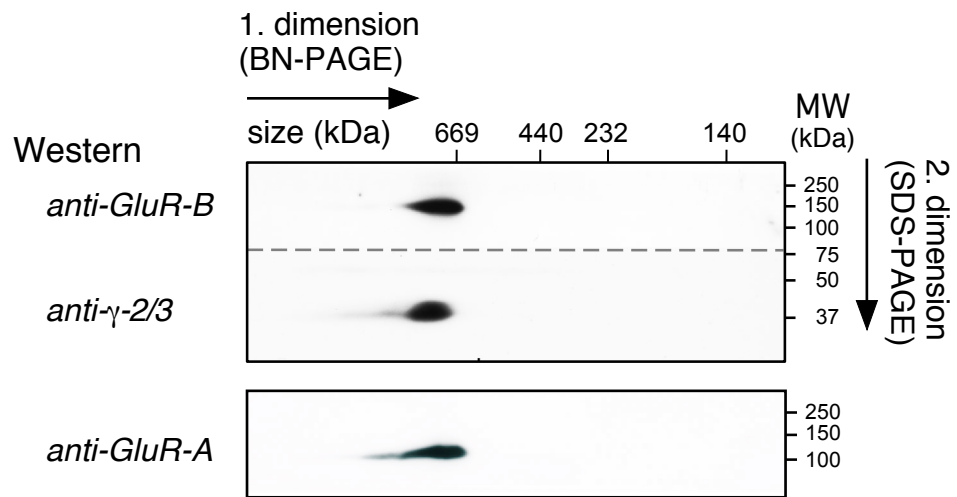
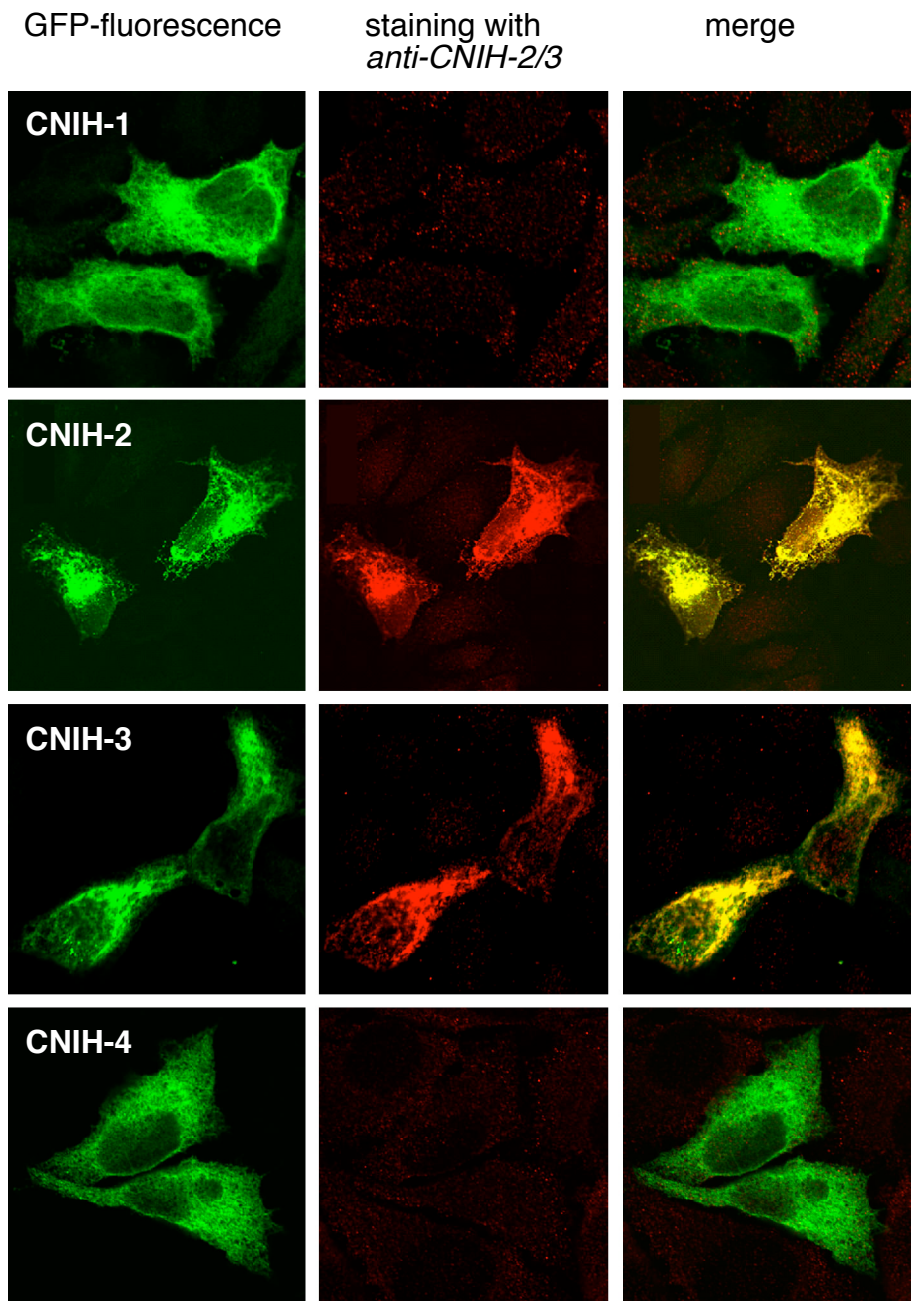
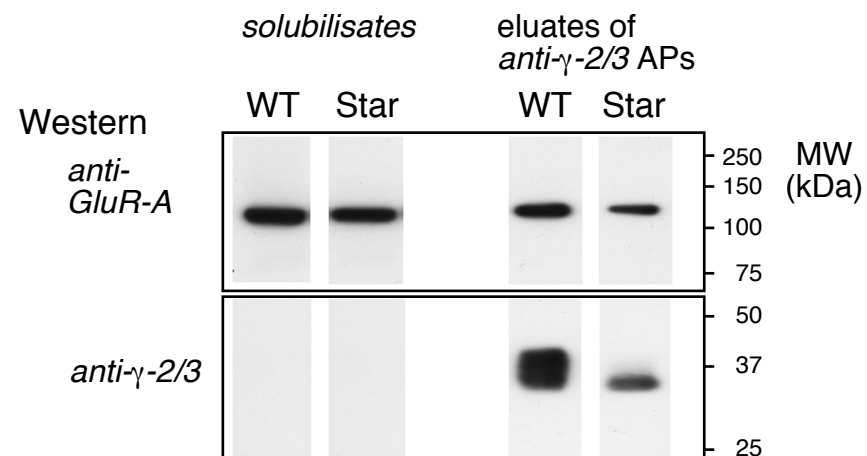


Figure S1, Schwenk et al.

A



B



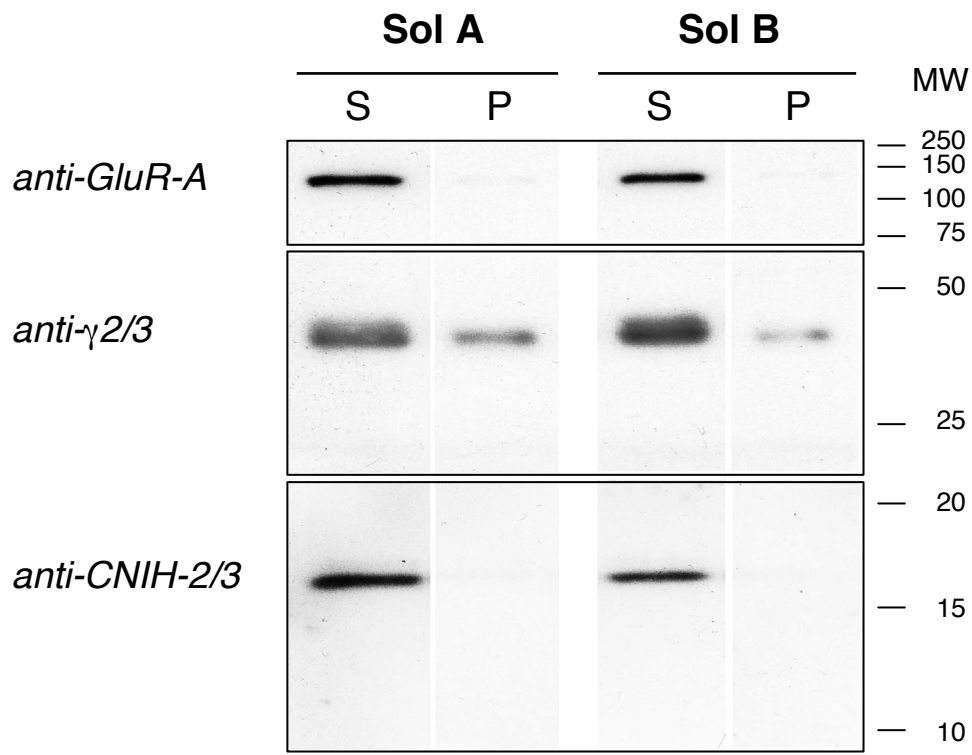
C

anti-gamma-2/3 AP

| Protein ID | WT mice | <i>stargazer</i> |
|-----------------------------------|--------------------|--------------------|
| | PQ _{norm} | PQ _{norm} |
| GluR-A | 0.92 | 1.02 |
| GluR-B | 2.30 | 2.87 |
| GluR-C | 1.32 | 1.54 |
| GluR-D | 1.12 | 1.05 |
| TARP γ-2 | 1.33 | 0.00 |
| TARP γ -3 | 1.60 | 1.40 |
| TARP γ -4 | 0.22 | 0.33 |
| TARP γ -5 | 0.00 | 0.00 |
| TARP γ -7 | 0.10 | 0.00 |
| TARP γ -8 | 0.23 | 0.31 |
| (CNIH-2) | 1.33 | 1.00 |
| (CNIH-3) | 0.33 | 0.67 |

Figure S2, Schwenk et al.

A



B

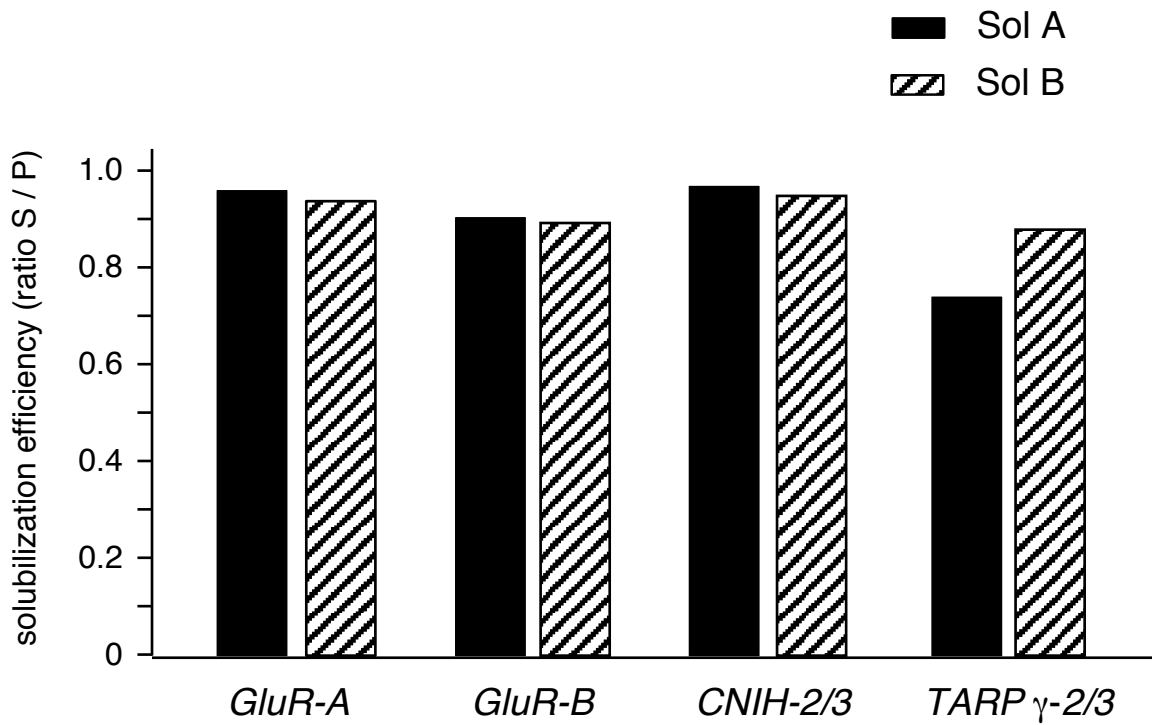
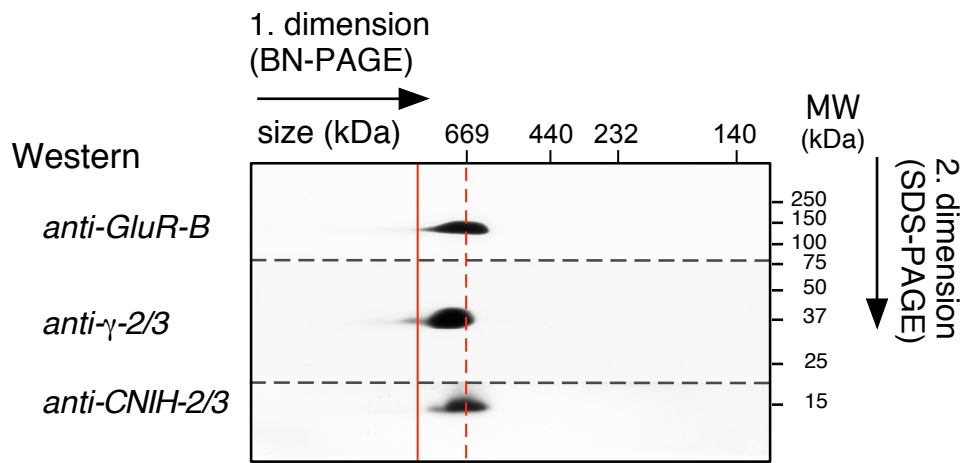


Figure S3, Schwenk et al.



AB-shift assay with *anti-CNIH-2/3*

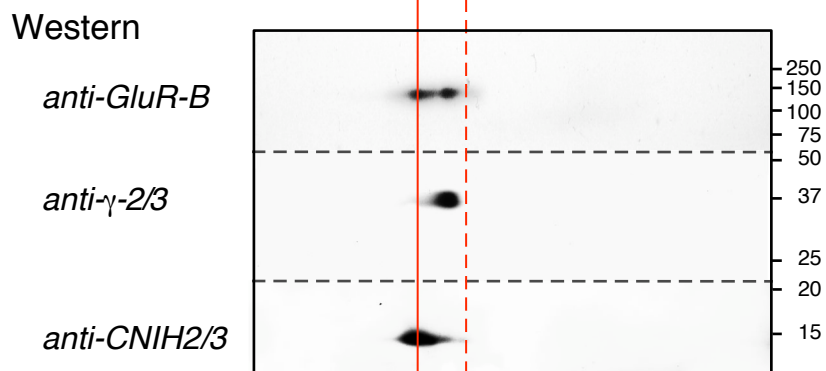


Figure S4, Schwenk et al.

A

native AMPARs: hilar mossy cells (hippocampus)

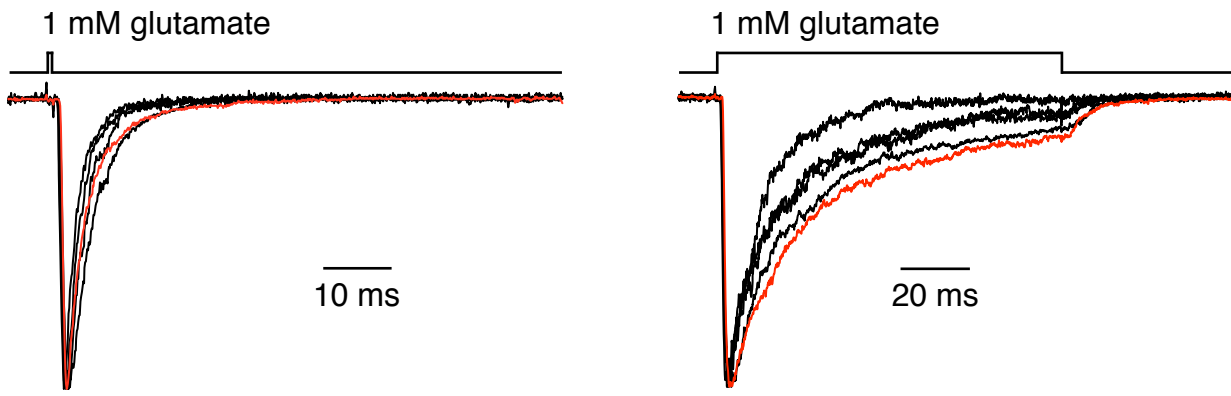
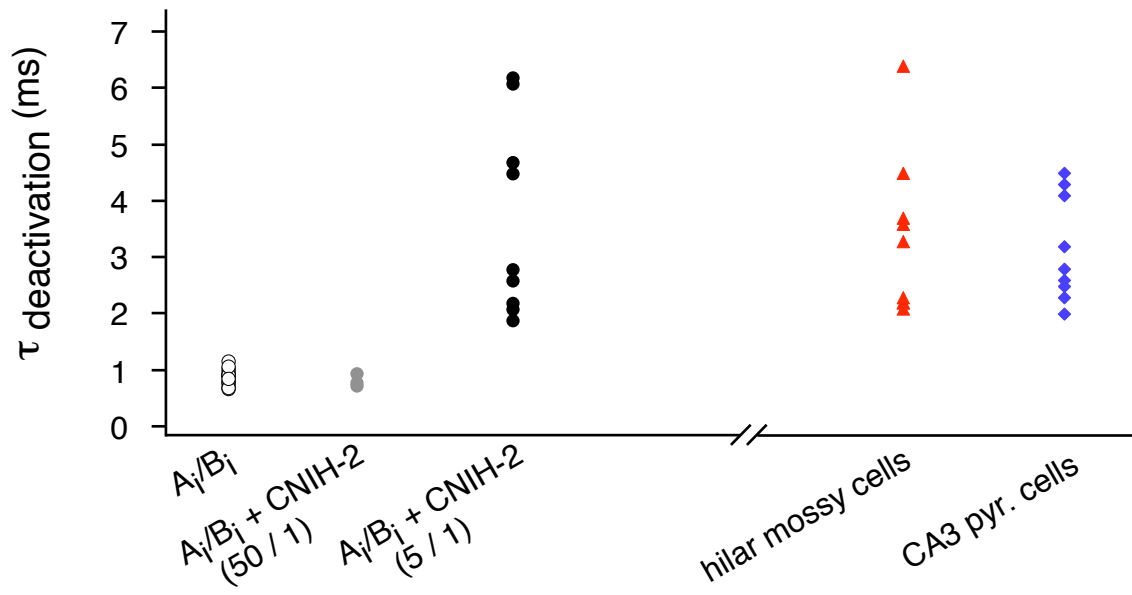
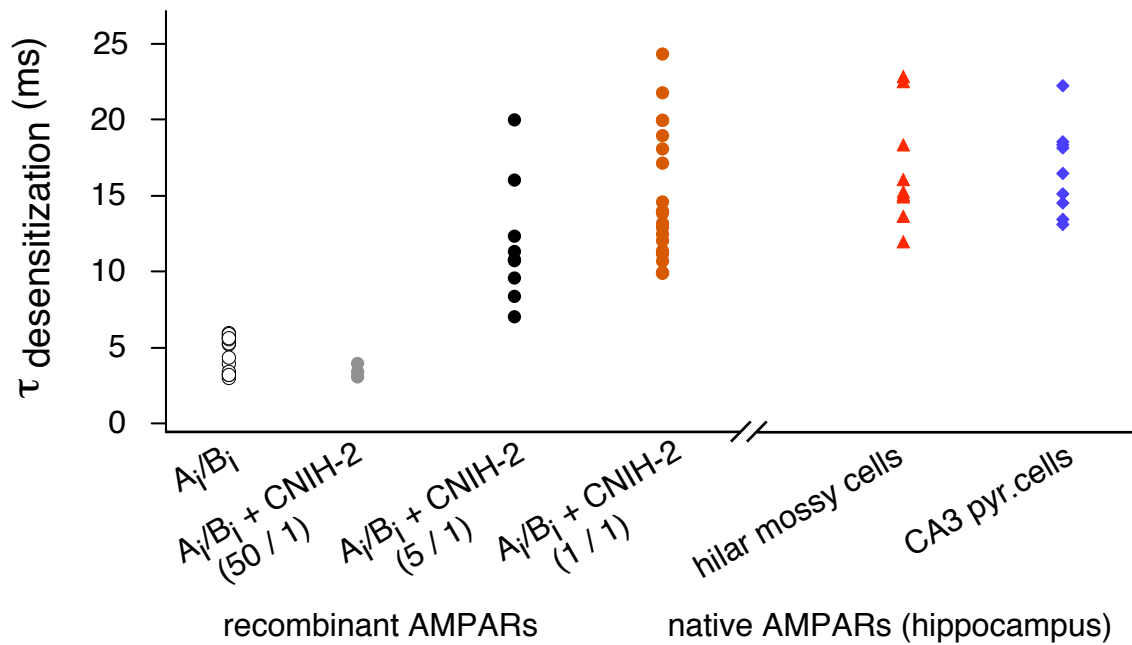
**B****C**

Figure S5, Schwenk et al.

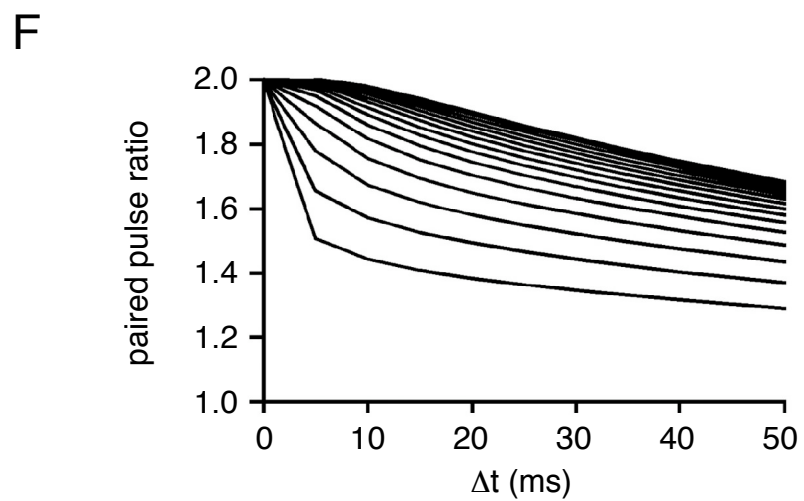
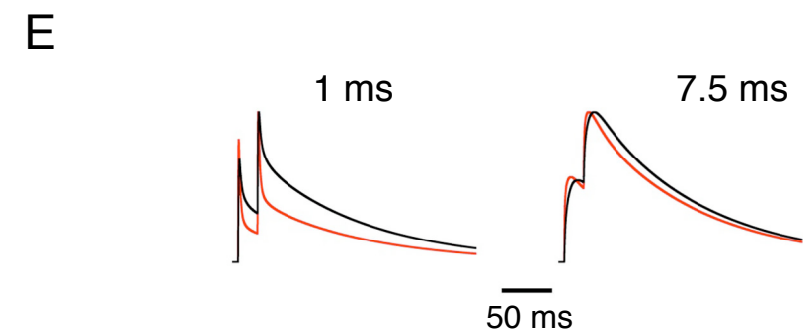
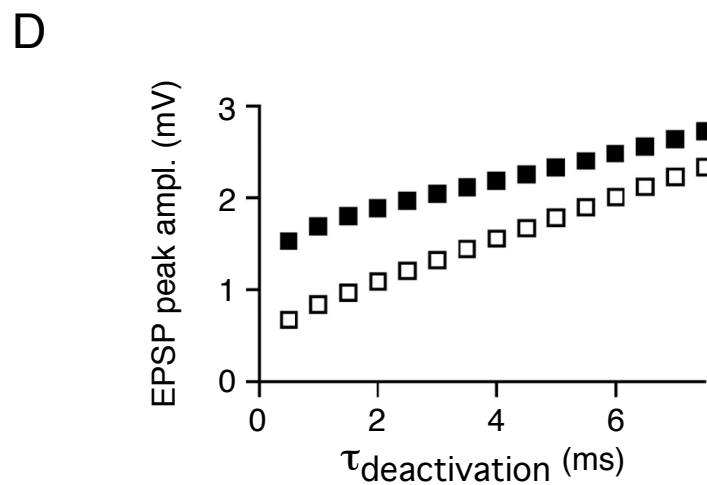
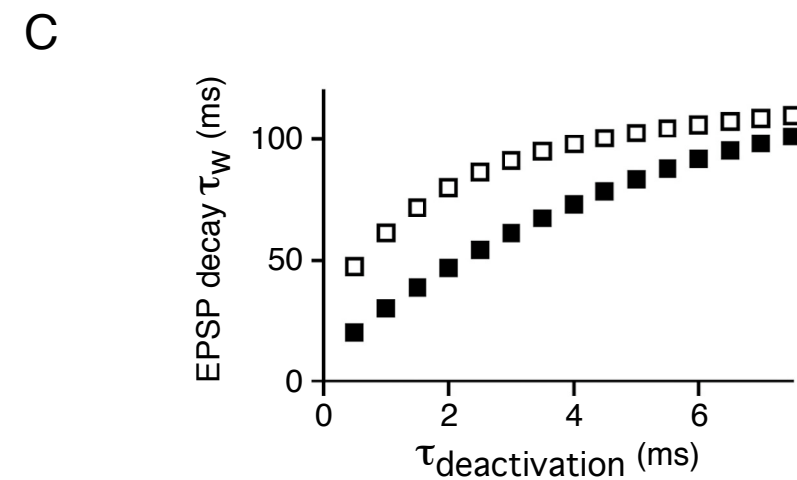
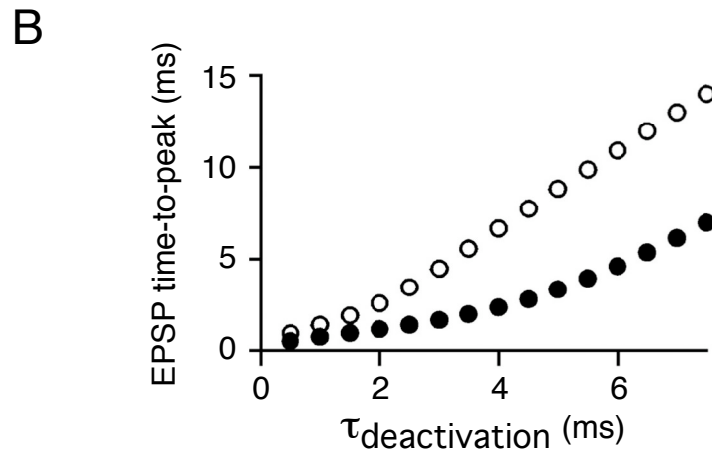
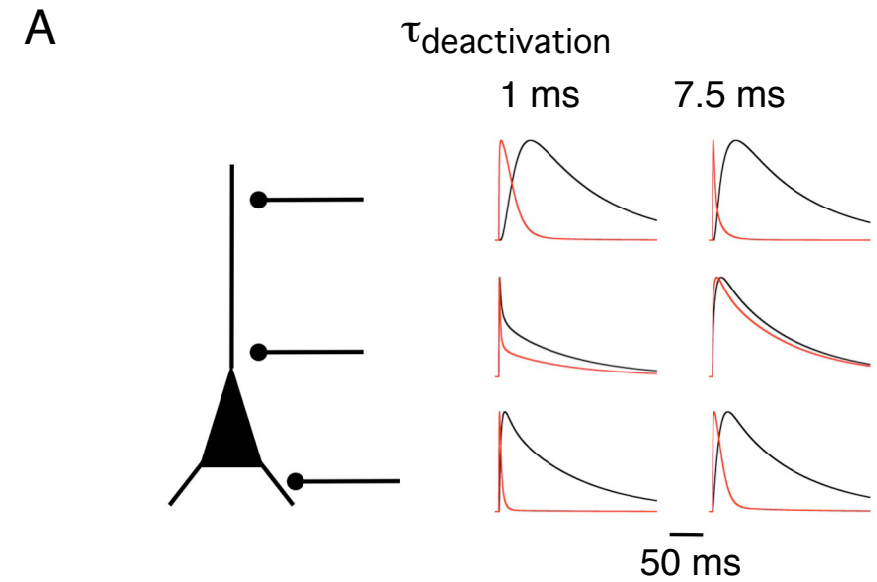


Figure S6, Schwenk et al.

| Protein ID | <i>anti-GluR-A</i> | | <i>anti-GluR-B</i> | | <i>anti-γ2/3</i> | | <i>anti-CNIH2</i> | |
|-----------------------------------|--------------------|--------------------|--------------------|--------------------|------------------------------------|--------------------|-------------------|--------------------|
| | rPQ | PQ _{norm} | rPQ | PQ _{norm} | rPQ | PQ _{norm} | rPQ | PQ _{norm} |
| GluR-A | 2144 | 5.58 | 2192 | 5.71 | 840 | 2.19 | 344 | 0.90 |
| GluR-B | 2888 | 8.21 | 5248 | 14.91 | 1680 | 4.77 | 608 | 1.73 |
| GluR-C | 968 | 2.95 | 2664 | 8.12 | 1144 | 3.49 | 368 | 1.12 |
| GluR-D | 880 | 2.56 | 1504 | 4.37 | 872 | 2.54 | 200 | 0.58 |
| TARP γ -2 | 88 | 0.92 | 240 | 2.50 | 176 | 1.83 | 24 | 0.25 |
| TARP γ -3 | 120 | 1.50 | 264 | 3.30 | 176 | 2.20 | 32 | 0.40 |
| TARP γ -4 | 16 | 0.22 | 40 | 0.56 | 56 | 0.78 | 8 | 0.11 |
| TARP γ -5 | 16 | 0.22 | 0 | 0.00 | 0 | 0.00 | 0 | 0.00 |
| TARP γ -7 | 40 | 0.50 | 40 | 0.50 | 8 | 0.10 | 0 | 0.00 |
| TARP γ -8 | 88 | 0.85 | 112 | 1.08 | 80 | 0.77 | 0 | 0.00 |
| cornichon homologue 2 (CNIH-2) | 176 | 7.33 | 288 | 12.00 | 56 | 2.33 | 64 | 2.67 |
| cornichon homologue 3 (CNIH-3) | 72 | 3.00 | 96 | 4.00 | 40 | 1.68 | 16 | 0.67 |

Table S1, Schwenk et al.